Analyst

Accepted Manuscript

This article can be cited before page numbers have been issued, to do this please use: J. Du , Q. Jiang, X. Lu, L. Chen, Y. Zhang and X. Xiong, *Analyst*, 2019, DOI: 10.1039/C8AN02049C.

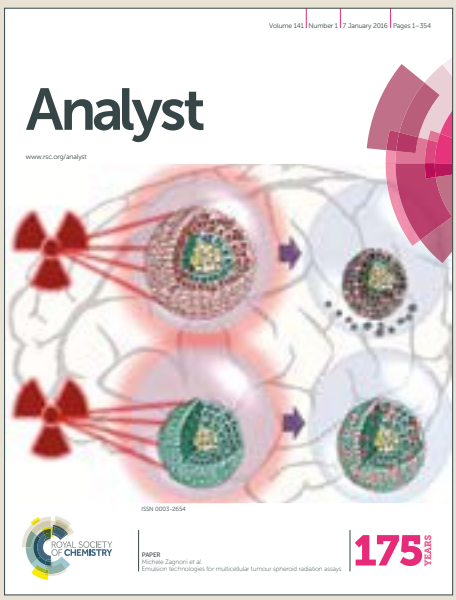

ROYAL SOCIETY OF CHEMISTRY

rsc.li/analyst

Journal Name

ROYAL SOCIETY OF CHEMISTRY View Article Online
DOI: 10.1039/C8AN02049C

ARTICLE

Detection of sulfadimethoxine using optical images of liquid crystals

JiaYin Du,[a]QiFeng Jiang,[a]XiaoChen Lu,[a]LongCong Chen,[a] Yan Zhang,[a]and XingLiang Xiong,*[a]

A label-free method for sulfadimethoxine (SDM) detection using aptamer-based liquid crystal biosensor is developed. The sensor probe is fabricated by immobilizing amine-functionalized aptamers onto the glass slide decorating mixed self-assembled layers of triethoxysilylbutyraldehyde (TEA) and N,-N-dimethyl-n-octadecyl-3-aminopropyltrimethoxysilylchloride (DMOAP). Liquid crystals (LCs) are supported on the surface and serve as response elements, which assume the homeotropic alignment and cause a dark optical appearance under crossed polarizers. In the presence of the SDM, the formations of SDM-aptamer compounds induce a notable change in the topographical structure of the surface, which disturb the original homeotropic orientation of LCs and result in a bright optical appearance. A detection limit of 10 μg/L is obtained, which is far lower than the maximum residue limit (100 μg/L in China). This facile method shows good specificity for SDM detection and may have great potential for detecting other small molecules.

1. Introduction

Sulfadimethoxine (SDM) has been used as a feed additive agent for the treatment and prevention of animal diseases due to its extensive antibacterial spectrum and high antibacterial activity. However, the abuse of SDM could lead to severe side effects, such as acute haemolytic anemia, which perniciously impacts human health.[1-5] Therefore much concern has been raised about SDM residues in meat, milk, eggs and other foods. The maximum residue limit of SDM in animal foods stipulated by the ministry of agriculture of China was 100 μg/L. Several approaches have been applied to detection of SDM, such as high-performance liquid chromatography (HPLC),[6] fluorescence analysis,[7]colorimetry,[8] and aptasensor[9], they exhibit specificity and sensitivity for SDM analysis. However, drawbacks still exist among these conventional methods, such as costly expense, cumbersome process, time-consuming and needing sophisticated instruments. Hence, it is imperative to establish a simple, effective and sensitive method for SDM detection.

Liquid crystals are materials that possess various superior properties, such as sensitive orientation response and optical anisotropy. The orientation of LCs are intensely sensitive to minute physical or chemical changes on the surfaces, and the orientation responses can be amplified to the bulk of LCs naturally due to weak intermolecular interaction forces between LC molecules[11-14]. This property is helpful for highly sensitive detection of biochemical binding events occurring on the surface without any other additional chemical or physical amplification technologies. Furthermore, the orientation response can perform within tens of milliseconds owing to their liquid-like mobility and the elastic force within LCs phase. It provides the possibility of rapid detection by using LCs. In addition, LC molecule is birefringent, therefore the orientation response can be easily visualized under crossed polarizers. This allows the use of LCs for naked-eye detection without any use of complex and expensive instruments. Thus, liquid crystals have been recognized as ideal materials to transduce chemical or biomolecular binding events into amplified visible optical signals in the sensing system.[15] Compared with traditional sensors, the liquid crystal-based biosensors have the advantages of simple operation, label-free, low cost, high sensitivity, making liquid crystal biosensors have been widely applied in the biochemical analysis, genetic test, and environmental monitoring.[16-22]

Aptamers, oligonucleotide fragments obtained from the nucleic acid molecular library by the index enrichment ligand system evolution technology (SELEX),[23-26] are ideal molecule recognition elements in the fabrications of sensors. Compared with antibodies, aptamers possess equivalent or higher specificity and affinity with their corresponding ligands. Furthermore, they also present other advantages over antibodies, including easy synthesis and modification, high stability and low cost, allowing aptamer to be an excellent substitution for antibody when used as a recognition molecule in sensors.[27-31]

In this paper, we have exploited a simple aptamer-based liquid crystal biosensor for detection of SDM by using liquid

View Article Online
DOI: 10.1039/C8AN02049C

crystals as signal transduction element. A mixed aptamer/DMOAP layer which immobilized on the surface of the glass slide is used to induce the homeotropic orientation of LCs. The optical signals are obtained when the homeotropic orientation of LCs is disrupted by specific binding events between SDM molecules and aptamers on the surface. The proposed sensing strategy represents a label-free, sensitive and selective method for detection of SDM.

.

2. Experimental

2.1. Materials and reagents

Glass slides were purchased from Xinhua Laboratory Glassware Company. Copper grids (20-μm thickness) were provided by Xian Zhongjingkeji Technology Co., Ltd. 4-cyano-4′-pentylbiphenyl (5CB) was obtained from Huajing Scientific and Technological Development Co., Ltd. SDM was provided by Sigma Aldrich. N,-N-dimethyl-n-octadecyl-3-amimopropyltrime -thoxysilylc-aminopropyltrimethoxysilylchloride (DMOAP) andtriethoxysilylbutyraldehyde(TEA) were obtained from Shanghai Yuanyekeji Technological Co., Ltd. Ampicillin, sulfadiazine sodium, streptomycin, kanamycin and glycine were purchased from Beijing solarbio technology Co., Ltd.Tetracycline and SDM aptamer (5'-NH_2-$(CH_2)_6$-GAGGGCAACGAGTGTTTATAGA-3',P1) were provided by Sangon Biotech Co., Ltd. Raw milk, honey and egg were purcha sed in a local market. All solvents were either analytical or HPLC grade, ultrapure water (18.25 MΩ) was used in experiments.

2.2. Cleaning of the glass slips

The glass slides (2.5 cm × 2.5 cm) were immersed in a freshly prepared piranha solution (70% H_2SO_4, 30% H_2O_2, v/v) at 80 °C for 1 h to remove the organic contaminants on the surfaces of glass slides, rinsed with copious amounts of deionized water, and then dried under a stream of nitrogen.

2.3. Preparation of DMOAP-modified glass slides

The cleaned glass slide was immersed in an ethanol solution containing 0.3% (v/v) DMOAP at room temperature (25 ± 2 °C) for 10 min, washed with ethanol and deionized water respectively, finally dried under a stream of nitrogen. The DMOAP-modified glass slide acted as top slide in following fabrication of LC cells.

2.4. Preparation of mixed TEA/DMOAP-modified glass slides

The other cleaned glass slide was immersed in an ethanol solution containing 1% (v/v) TEA and 0.3% (v/v) DMOAP at 50°C for 1 h, rinsed with ethanol and deionized water respectively, finally dried under nitrogen. The slide acted as the bottom slide (work slide) in following fabrication of LC cells.

2.5. Immobilization of aptamer on glass slides

Amine-modified aptamers (**P1**) were dissolved in the buffer solution (20 mM Tris-HCl, 10 mM $MgCl_2$, pH = 7.4), then the aptamer solution (200 μL, 100 nM) were spotted onto the TEA/DMOAP-coated substrate. After 12 h of incubation at 37 °C, the glass slides were rinsed in buffer solution (2 × SSC, 0.3 M NaCl, pH=7.0) that containing 0.1% (v/v) SDS. Dried the slides under nitrogen.

2.6. Fabrication of LC cells

The copper grids were washed with ethanol and deionized water separately, dried under nitrogen. After heated at 110 °C for 1 h, the grids were placed onto the work slides decorated with various molecules (TEA/DMOAP, TEA/DMOAP/P1, TEA/DMOAP/P1/SDM). 2 μL of 5CB（40 °C） was added onto each grid, and the excess 5CB was removed from the grid with a clean capillary tube. Then placed a top slide onto the work slide and secured them with binder clips.

2.7. Detection of SDM

In order to screen unreacted aldehyde groups of the TEA molecules, firstly we submerged the TEA/DMOAP/P1-coated glass slides in glycine solution (80 mM) at room temperature (25 ± 2 °C) for 1 h, then washed the slides with deionized water and dried them under nitrogen. After an immersion of 6 h at room temperature (25 ± 2 °C) in SDM solutions with different concentrations, the glass surfaces were repeatedly washed with deionized water and dried under nitrogen, then fabricated LC cells in accordance with the method described above. Finally, The LC cells were placed on a polarizing microscope with crossed polarizers. Optical images of LC cells were captured by a digital camera mounted on the microscope and average gray values of the optical images were calculated by using Adobe PhotoShop software.

2.8. Atomic force microscope (AFM) characterization of the film on the surfaces

The surface topographies of the slides respectively modified w ith 1% (v/v) TEA, 0.3% (v/v) DMOAP, 1% (v/v) TEA / 0.3% (v/v) DMOAP, 1% (v/v) TEA / 0.3% (v/v) DMOAP / 200 nM P1 and 1% (v/v) TEA / 0.3% (v/v) DMOAP / 200 nM P1 / 100 μg/L SDM we re performed using an atomic force microscope (AFM, Dimensi on ICON, Bruker) by ScanAsyst Mode.

2.9. Water contact angle measurement

Water contact angles were tested by the contact angle meter (GBX, France). Droplets of deionized water (5 μL) were carefully injected onto the glass surfaces coated with different self-assembled layers (TEA, TEA/DMOAP, DMOAP), then images of the droplets were captured from which water contact angles were obtained.

View Article Online
DOI: 10.1039/C8AN02049C

2.10. Real sample preparation

Raw honey was diluted ten times with phosphate buffer solution (0.0l M, pH = 7.4). Raw milk was dissolved in deionized water. The egg was homogenized. Then experiments were carried out on the three kinds of samples: added 5 ml acetonitrile to 1 ml sample solution, the mixture was centrifuged at 3000×g for 10 min to separate the precipitates. All the supernatants were dried under vacuum, dissolved with 1 ml phosphate buffer solution and mixed with 1 ml heptane. After three times of centrifugation, decanted the water phase and stored it at 4 °C.

3. Results and discussion

3.1. Sensing strategy for detection of SDM

The sensing strategy of the presented LCs-based biosensor is illustrated in Figure 1. A mixed self-assembled film of TEA/DMOAP coated on the glass slide (Fig. 1a) possesses dual functions. The DMOAP molecules, known as orientation agents for LC molecules, are used to induce homeotropic orientation of LCs supported on the slide. In contrast, The TEA molecules, containing active aldehyde groups, act as linker agents to bind amine-modified aptamers onto the glass slide (Fig. 1b). The LC molecules adopt homeotropic orientation on the slide when rational controlling the TEA/DMOAP ratio and the amounts of aptamers immobilized on the slide. With the synergistic effect of the DMOAP molecules immobilized on another slide, the bulk of thin LC film (~20 μm thickness) will assume homeotropic orientation (Fig. 1d), thus the polarized image appears uniform dark through crossed polarizers (Fig. 1f).In the presence of SDM, the formations of compounds between SDM molecules and the aptamers supported on the glass slide due to specific molecular recognition, will change the spatial conformation of the film immobilized on the glass slide (Fig. 1c), thus distort the original homeotropic orientation of LCs (Fig. 1e). In turn, this orientational transition causes the polarized image changes from dark to bright (Fig. 1g). Therefore, this system can transduce the biological binding events occurring on the surfaces into the response of the polarized lights signal, which can be observed by bare eyes without other advanced instruments.

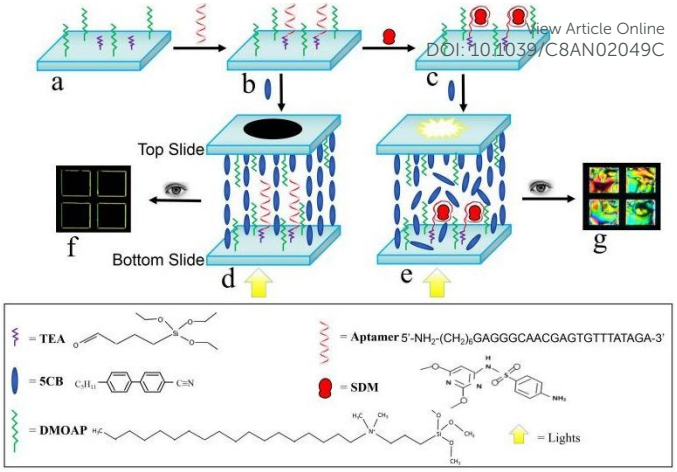

Fig. 1 Schematic illustration of aptamer-based LC biosensor for SDM

3.2. Effects of the TEA/DMOAP (v/v) ratio on the orientation of LCs

Previous studies have demonstrated that the chemical compositions of films coated on the surface and their topography have a great influence on the orientation of LCs[32]. Therefore, we first inspected the orientation behavior of LCs on the surface modified with different ratios of TEA/DMOAP. The optical images under crossed polarizers change from bright to dark with the decrease of TEA/DMOAP ratio (Fig.2.1),indicating that the LC molecules suffer an orientation transition from planar to homeotropic gradually. A uniform dark background appears when the TEA/DMOAP ratio reduces to 3:1 or lower (Fig.2.1e-f), which suggests that the LCs assume uniform homeotropic orientation on these surfaces. The homeotropic orientation of LCs is mainly directed by the nanometer-scale topographical structure of the film, in the absence of the short-range force such as hydrogen bond and coordination interaction between the LC molecules and the film. The largest peak-to-valley-height (LPVH) of the film greater than the length of LC molecule (~2 nm for 5CB) is a necessary condition to ensure a homeotropic orientation of LCs[33]. Our atomic force microscope (AFM) images (Fig. 2.2b-c) confirmed this conclusion. The TEA-coated surface with the height of ~1.6 nm (Fig. 2.2a), is unable to induce a homeotropic orientation of 5CB. Water contact angle test (Fig. 2.3) of the films further confirms that the film modified withTEA/DMOAP can induce the homeotropic orientation of LCs when they possess sufficient hydrophobicity. Our results are reasonable agreement with a past study which found that 5CB assumed a homeotropic orientation when the water contact angle of the film was greater than 64°[34]. It is worth noting that although the water contact angle of TEA film (66.5°) greater than 64°, they cannot induce a homeotropic orientation of 5CB. This is because the TEA film has a relatively small LPVH (~1.6 nm) which is unfavorable for homeotropic orientation of 5CB. Reducing the TEA/DMOAP ratio has little effect on the hydrophobic properties of the substrate, it will reduce the coverage of the aldehyde group, which is not beneficial for aptamers immobilization. On the premise of

ensuring the homeotropic orientation of LCs, a higher TEA/DMOAP ratio means more aptamers can be immobilized on the glass slide, which is beneficial for lowering the detection limit of the sensors. Therefore, the TEA/DMOAP ratio of 3:1 is employed in further experiments.

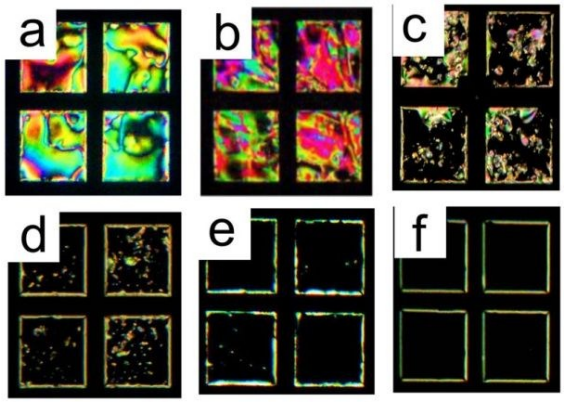

Fig. 2.1 Effect of TEA/DMOAP films on the orientation of LC. The surface of the glass slide was self-assembled with mixed 1% (v/v) TEA and 0.3% (v/v) DMOAP, the ratio(v/v)of TEA/DMOAP was: (a) 20:1; (b) 10:1; (c) 7:1; (d) 5:1; (e) 3:1; (f) 2:1, respectively.

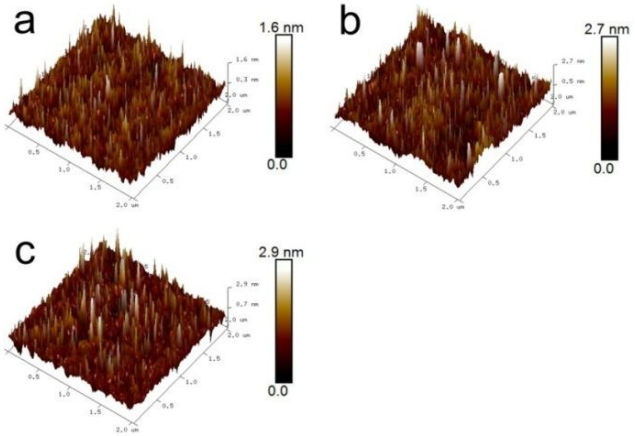

Fig. 2.2 AFM characterization images of substrates coated with: (a) 1% (v/v) TEA; (b) 1% (v/v) TEA and 0.3% (v/v) DMOAP, the ratio (v/v) of TEA/DMOAP was 3/1; (c) 0.3% (v/v) DMOAP.

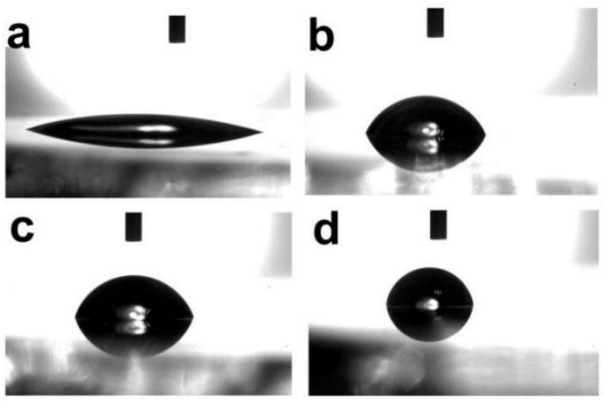

Fig. 2.3 Water contact angle characterization of different substrates: (a) Glass slide: 15.8°; (b) Slide coated with 1% (v/v) TEA: 66.58; (c) Slide coated with 1% (v/v) TEA and 0.3% (v/v) DMOAP with the ratio was 3/1: 75.1°; (d) Slide coated with 0.3% (v/v) DMOAP: 87.3°

3.3. Effects of the aptamers on the orientation of LCs

In order to ensure the LCs remain homeotropic orientation before using to detect SDM, we further examined the effect of the aptamers modified on the TEA/DMOAP-coated slides on the orientation of LCs. The results show that the optical appearances change from bright to dark with the decreasing of aptamer concentrations (Fig. 3), which demonstrates that the LCs suffer the planar-to-homeotropic transition. The LCs adopt the homeotropic orientation while the concentration of aptamer immobilized on the glass slides is about 200 nM (Fig. 3d), indicating that appropriate amounts of aptamers will not disturb the original orientation of LCs. Based on these observations, we propose that 200 nM is the optimal one for the following experiments in order to ensure enough quantities of aptamers to immobilize on the glass slides.

3.4. Sensitivity

To investigate the feasibility of the presented method for detection of SDM, we prepared a series of LC cells with their slides were incubated with different concentrations of SDM. The resultant optical images of the LC cells are shown in Figure 4. The bright areas in the images become smaller with the concentrations of SDM decreasing from 100 μg/L to 10 μg/L (Fig. 4a-e), indicating that the formations of SDM-aptamer compounds on the glass slides are capable of disturbing the homeotropic orientation of LCs. The smaller the amount of SDM-aptamer complex formed on the slides, the less obvious the orientation transition. We attribute the orientation transition of LCs to the changes of the surface topography of the slides due to specific binding between SDM molecules and aptamers occurred on the surface. This conclusion can be confirmed by AFM images. Comparison with the surface topography before binding with SDM (Fig. 4h), great changes of the topography took place on the surface after binding with SDM (Fig. 4i). The optical appearance assumes a uniform dark when the concentration of SDM is reduced to about 5 μg/L (Fig. 4f). This result suggests that small amounts of SDM-aptamer compounds on the surface could not enough to disrupt the homeotropic orientation of LCs due to an insignificant change of surface topography. SDM concentration was taken logarithm separately and then fitted curve tracing with the average brightness value of the corresponding optical image. Fig. 4g presents that a linear relationship between the average gray value and SDM concentration. The average gray value increases with the SDM concentration improving. The plot of the average gray values as a function of the SDM concentrations between 10 μg/L - 200 μg/L exhibited linear relationship with a high correlation coefficient (R^2) of 0.9825, suggesting that the quantitative analysis of SDM concentrations could be achieved by this liquid crystal biosensor below 200 μg/L and the detection limit of SDM in our study is about 10 μg/L.As far as the detection

limit, our method for SDM analysis is better than those other methods reported before (Table 1), suggesting that the proposed biosensor has the superiority on sensitive detection of SDM.

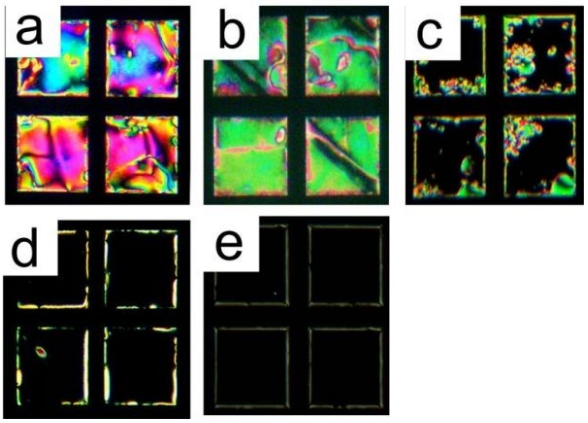

Fig. 3 Effect of aptamers on the orientation of LCs. The aptamers were immobilized on the TEA/DMOAP-modified surfaces at the concentration of: (a)700 nM; (b)500 nM; (c)300 nM; (d)200 nM; (e)100 nM, respectively.

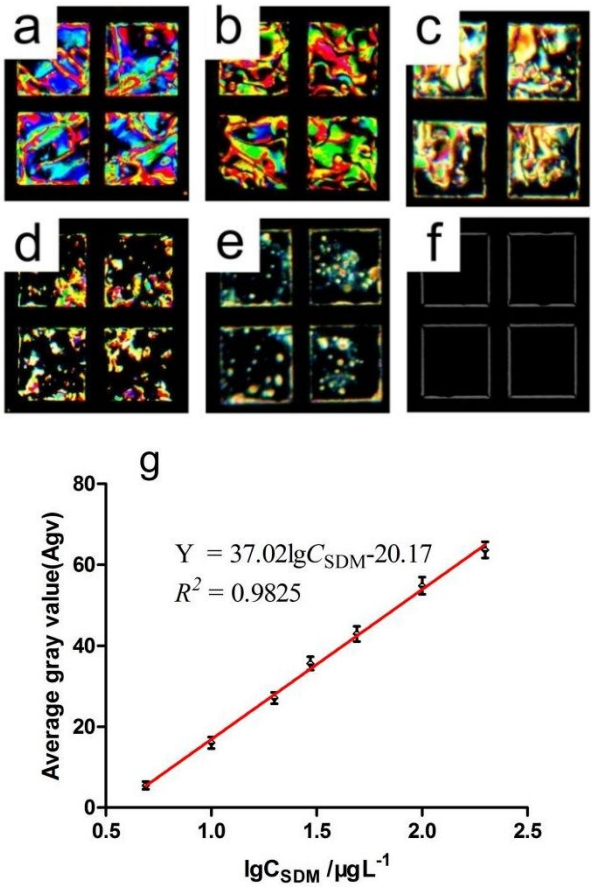

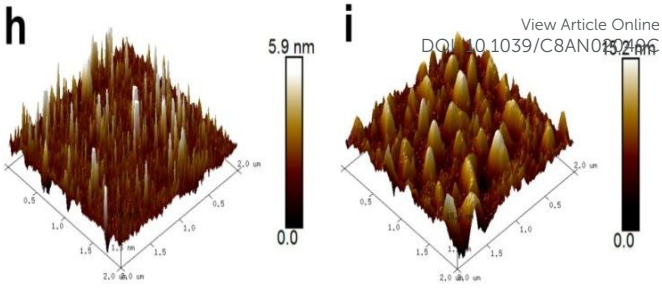

Fig. 4 The optical images of 5CB supported on the substrates with SDM at the concentration of: (a) 100μg/L; (b) 50μg/L; (c) 30μg/L; (d) 20μg/L; (e) 10μg/L; (f) 5μg/L; (g) The corresponding linear calibration curve of the average gray value of the optical image vs the logarithm of the SDM concentration (C_{SDM} is the concentration of SDM, Y is the average gray value of the optical image, n = 3); (h) AFM result of surface modified with 200 nM aptamer; (i) AFM result of surface modified with compounds induced by reaction between SDM (100 μg/L) and aptamer (200 nM).

Table 1. Various methods for the determination of SDM

Methods	Limit of Detection	Reference
HPLC	94.7 μg/kg	6
Fluorescence	25 μg/L	7
Colorimetric	500 μg/L	8
Label-free apatasensor	50μg/L	9
Electrochemical	21.7μg/L	10
Liquid crystal biosensor	10 μg/L	This work

3.5. Specificity

We selected several typical antibiotics such as sulfadiazine, streptomycin, penicillin, kanamycin and tetracycline as control groups to investigate the specificity of the LC-based biosensor. The solutions of SDM and the above antibiotics at the same concentration (100 μg/L) were incubated on the DMOAP/TEA/P1-coated slides, respectively. Then a series of LC cells were prepared. The optical images of the LC cells were obtained by polarizing microscope. As shown in Figure 5, the optical image assumes bright (Fig. 5a) when SDM incubate on the slide. On the contrary, the optical images appear dark (Fig. 5b-f) while other antibiotics incubate on the slide. These results suggest that no biological binding events occurred on the slides except incubation with SDM. It is worth noting that the molecular structure of sulfadiazine is very similar to that of SDM, but it still cannot bind with the aptamers. That means SDM molecules can bind to the aptamers on the glass slides with high affinity and specificity. The small bright spots in the

optical images (Fig. 5b-f) may be originated from the insufficient wash of uncombined molecules.

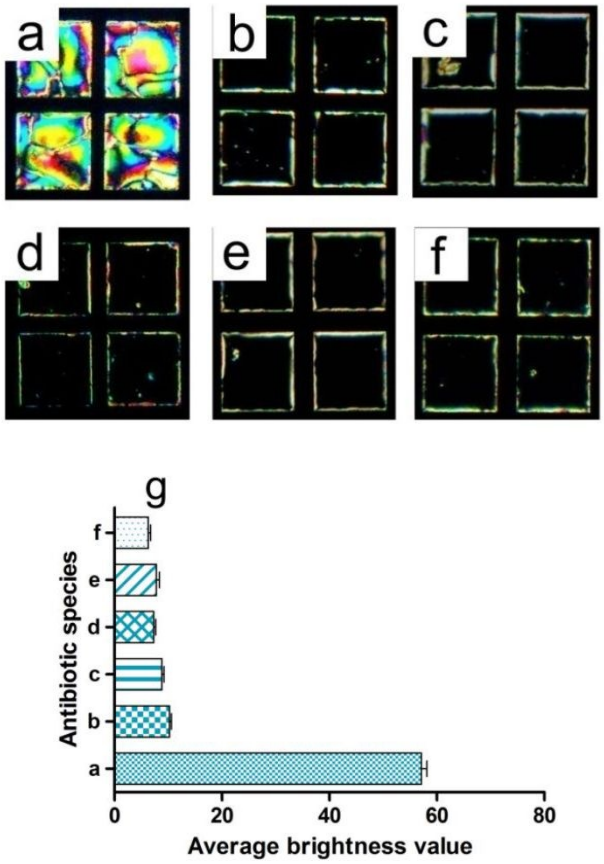

Fig. 5 Obtained optical images under several conditions: (a) SDM; (b) sulfadiazine sodium; (c) streptomycin; (d) penicillin sodium; (e) Kanamycin; (f) tetracycline; (g) Corresponding average brightness values.

3.6. Real sample analysis

We finally employed the biosensor to detect SDM in real food samples. Raw milk, honey, and egg were purchased in a local market and pretreated according to the method in 2.8. Deionized water (DI water) served as the blank sample. Measurements were carried out in triplicate. As is shown in Figure 6, the average gray values of optical signals among the animal-derived food groups are nearly close to that of DI water group, suggesting that these food samples contain very little residual SDM. The result indicates that the developed biosensor is successfully applied to detect SDM in animal-derived food samples.

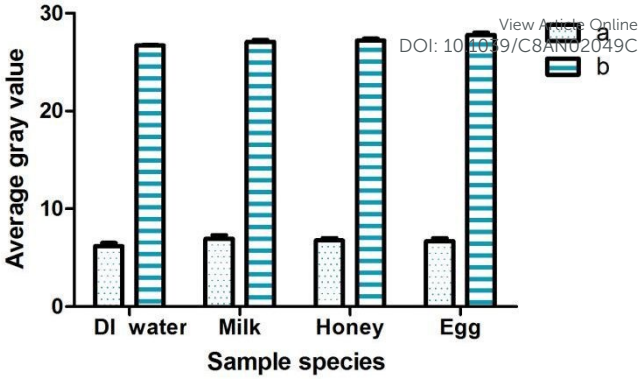

Fig. 6 Average gray values of optical signals for real samples detection: (a) Before adding SDM into real samples; (b) After adding 20 μg/L SDM into real samples.

4. Conclusions

In summary, we have successfully demonstrated a simple detection assay for SDM with high sensitivity and specificity. The principle of SDM detection is based on the orientation transition of LCs driven by the binding of SDM molecules to aptamers immobilized on the aldehyde-coated surface. This binding event occurred on the glass slide can change the surface topography and induce a homeotropic-to-parallel transition of the orientation in LC cell, which can be easily visualized through the crossed polarizers. This sensor system shows good specificity and reaches a low detection limit of 10 μg/L. Furthermore, the technique proposed here is also available for the detection of other biological molecules with high specificity when immobilized their aptamers onto the surface of glass slides.

Conflicts of interest

The author(s) declare that they have no competing interests.

Acknowledgements

This research is funded by Chongqing Research Program of Basic Research and Frontier Technology (cstc2018jcyjAX0165).

Notes and references

1. N. Mosleh, M. Ashrafi, T. Shomali, N. Mobarraei and N. Ahmadi, *International Journal of Toxicological & Pharmacological Research*, 2016, **8**, 430-433.
2. X. Liu, T. Gao, X. Gao, T. Ma, Y. Tang, L. Zhu and J. Li, *Microchimica Acta*, 2017, **184**, 3557-3563.
3. J. Savel, *Therapie*, 1960, **15**, 952-966.
4. J. Y. Park and B. Huwe, *Environ Sci Pollut Res Int*, 2016, **23**, 12456-12466.
5. C. F. Peng, X. H. Duan, Q. L. Pan, L. Q. Liu and F. Xue, *Journal of Chemistry,2013,(2013-12-29)*, 2013, **2013**, 1-5.
6. E. Karageorgou, N. Manousi, V. Samanidou, A. Kabir and K. G. Furton, *Food Chemistry*, 2016, **196**, 428-436.
7. T. Bing, H. Zhao, D. Lei, X. Gan and Q. Xie, *Biosensors & Bioelectronics*, 2016, **83**, 267-273.

View Article Online
DOI: 10.1039/C8AN02049C

8. S. Niu, Z. Lv, J. Liu, W. Bai, S. Yang and A. Chen, *Plos One*, 2014, **9**, e109263.
9. A. Chen, X. Jiang, W. Zhang, G. Chen, Y. Zhao, T. M. Tunio, J. Liu, Z. Lv, C. Li and S. Yang, *Biosensors & Bioelectronics*, 2013, **42**, 419-425.
10. A. Turco, S. Corvaglia and E. Mazzotta, *Biosensors & Bioelectronics*, 2015, **63**, 240-247.
11. R. J. Carlton, J. T. Hunter, D. S. Miller, R. Abbasi, P. C. Mushenheim, L. N. Tan and N. L. Abbott, *Liquid Crystals Reviews*, 2013, **1**, 29-51.
12. D. S. Miller, R. J. Carlton, P. C. Mushenheim and N. L. Abbott, *Langmuir*, 2013, **29**, 3154-3169.
13. J. S. Park and N. L. Abbott, *Advanced Materials*, 2010, **20**, 1185-1190.
14. S. Sivakumar, K. L. Wark, J. K. Gupta, N. L. Abbott and F. Caruso, *Advanced Functional Materials*, 2010, **19**, 2260-2265.
15. Y. Bai and N. L. Abbott, *Langmuir the Acs Journal of Surfaces & Colloids*, 2010, **27**, 5719-5738.
16. Y. Wang, B. Wang, J. Shen, X. L. Xiong and S. X. Deng, *Microchimica Acta*, 2017, **184**, 1-7.
17. S. Yang, C. Wu, H. Tan, Y. Wu, S. Liao, Z. Wu, G. Shen and R. Yu, *Analytical Chemistry*, 2013, **85**, 14-18.
18. J. Shen, F. J. He, L. C. Chen, L. Ding, H. L. Liu, Y. Wang and X. L. Xiong, *Microchimica Acta*, 2017, **184**, 3137-3144.
19. S. Liao, H. Ding, Y. Wu, Z. Wu, G. Shen and R. Yu, *Biosensors & Bioelectronics*, 2016, **79**, 650-655.
20. Z. Hussain, C. Zafiu, S. Küpcü, L. Pivetta, N. Hollfelder, A. Masutani, P. Kilickiran and E. K. Sinner, *Biosensors & Bioelectronics*, 2014, **56**, 210-216.
21. S. Liao, Y. Qiao, W. Han, Z. Xie, Z. Wu, G. Shen and R. Yu, *Analytical Chemistry*, 2012, **84**, 45-49.
22. J. Kim, M. Khan and S. Y. Park, *Acs Applied Materials & Interfaces*, 2013, **5**, 13135-13139.
23. S. Tombelli, M. Minunni and M. Mascini, *Biosensors & Bioelectronics*, 2005, **20**, 2424-2434.
24. S. C. Gopinath, *Analytical & Bioanalytical Chemistry*, 2007, **387**, 171-182.
25. Z. Zhuo, Y. Yu, M. Wang, J. Li, Z. Zhang, J. Liu, X. Wu, A. Lu, G. Zhang and B. Zhang, *International Journal of Molecular Sciences*, 2017, **18**, 2142.
26. C. Marimuthu, T. H. Tang, J. Tominaga, S. C. Tan and S. C. Gopinath, *Analyst*, 2012, **137**, 1307-1315.
27. F. Pfeiffer and G. Mayer, *Frontiers in Chemistry*, 2016, **4**, 25.
28. M. Jarczewska, Ł. Górski and E. Malinowska, *Analytical Methods*, 2016, **8**, 3861-3877.
29. U. Schlecht, A. Malavé, T. Gronewold, M. Tewes and M. Löhndorf, *Analytica Chimica Acta*, 2006, **573**, 65-68.
30. H. Sun, W. Tan and Y. Zu, *Analyst*, 2015, **141**, 403.
31. M. Yüce, N. Ullah and H. Budak, *Analyst*, 2015, **140**, 5379-5399.
32. S. Yang, Y. Liu, H. Tan, C. Wu, Z. Wu, G. Shen and R. Yu, *Chemical Communications*, 2012, **48**, 2861-2863.
33. S. L. Lai, S. Huang, X. Bi and K. L. Yang, *Langmuir the Acs Journal of Surfaces & Colloids*, 2009, **25**, 311-316.
34. A. D. Price and D. K. Schwartz, *Langmuir the Acs Journal of Surfaces & Colloids*, 2006, **22**, 9753-9759.

View Article Online
DOI: 10.1039/C8AN02049C

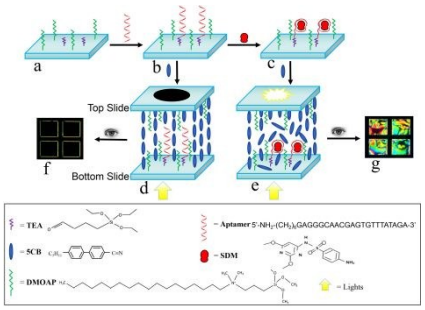

An aptamer based liquid crystal biosensor was firstly developed for sulfadimethoxine detection achieving a lower detection limit of 10 μg/L.